HHS Public Access

Author manuscript

J Memb Sci. Author manuscript; available in PMC 2021 April 01.

Published in final edited form as:

J Memb Sci. 2020 April 1; 599: . doi:10.1016/j.memsci.2020.117821.

Thermo-responsive adsorption-desorption of perfluoroorganics from water using PNIPAm hydrogels and pore functionalized membranes

Anthony Saad[a], **Rollie Mills**[a], **Hongyi Wan**[a], **M. Abdul Mottaleb**[b], **Lindell Ormsbee**[c], **Dibakar Bhattacharyya**[a,*]

[a]Department of Chemical and Materials Engineering, University of Kentucky, Lexington, Kentucky 40506-0046

[b]College of Medicine, University of Kentucky, Lexington, Kentucky 40506-0046

[c]Department of Civil Engineering, University of Kentucky, Lexington, Kentucky 40506-0046

Abstract

Perfluorochemicals (PFCs) are emerging contaminants in various water sources. Responsive polymers provide a new avenue for PFC adsorption/desorption from water. Poly-N-isopropylacrylamide's (PNIPAm's) temperature-responsive behavior and hydrophilic/hydrophobic transition is leveraged for reversible adsorption and desorption of PFCs. Adsorption of PFOA (perfluoro-octanoic acid) onto PNIPAm hydrogels yielded Freundlich distribution coefficients (K_d) of 0.073 L/g at 35 °C (above LCST) and 0.026 L/g at 22°C. Kinetic studies yielded second order rate constants (k_2) of 0.012 g/mg/h for adsorption and 12.6 g/mg/h for desorption, with initial rates of 28 mg/g/h and 41 mg/g/h, respectively. Interaction parameters of PNIPAm's functional groups in its different conformational states, as well as the hydrophobic fluorinated carbon tails and hydrophilic head groups of PFOA are used to describe relative adsorption. Polyvinylidene difluoride (PVDF) provides a robust membrane structure for the commercial viability of polymeric adsorbents. Temperature swing adsorption of PFOA using PNIPAm functionalized PVDF membrane pores showed consistent adsorption and desorption capacity over 5 cycles. PFOA desorption percentage of 60% was obtained in pure water at temperatures below PNIPAm's lower critical solution temperature (LCST) while 13% desorption was obtained at temperatures above the LCST, thus showing the importance of the LCST on desorption performance.

Graphical abstract

*Corresponding author: Dibakar Bhattacharyya, University Alumni Chair Professor, Chemical and Materials Engineering, 177 FPAT Bldg. University of Kentucky, Lexington, KY 40506, Phone: 859-312-7790; db@uky.edu.

Author Statement

Anthony Saad: Experiments, Manuscript writing; **Rollie Mills:** Characterization experiments, manuscript editing; **Hongyi Wan:** Reviewing and editing, Material Characterization; **M. Abdul Mottaleb**: Analytical methods, Data Analysis, Editing; **Lindell Ormsbee**: Reviewing and editing; **Dibakar Bhattacharyya**: Conceptualization, Manuscript writing and editing

Conflict of Interest

The authors declare no conflict of interest.

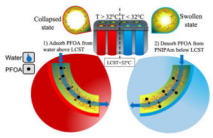

Keywords

water detoxification; PNIPAm; adsorption; PFOA; PFOS; hydrogel

1. Introduction:

Perfluorinated compounds (PFCs) such as Perfluorooctanoic acid (PFOA) have gained much attention as emerging pollutants due to their environmentally persistent nature and toxicity concerns that threaten water safety [1]. Due to their thermal stability, these highly hydrophobic compounds have been used since the 1960s for a variety of purposes including: protective coatings, lubricants, surfactants, additives, and repellants. Methods to remove them from contaminated wastewater, groundwater, and drinking water continue to gain importance due to their continued production and toxicity [2–4]. PFC concentrations in contaminated wastewater and groundwater samples range from below 0.1ng/L to over 1000 mg/L values [4–6]. To date, various methods have been explored for the removal of PFCs from aqueous media, such as reverse osmosis [7], incineration [8], anaerobic defluorination [9], photochemical defluorination [10], oxidation[11], reduction [12], electrostatic exclusion by nanofiltration [13], and adsorption [14–17]. The current advised US EPA level for PFCs is 70 ng/L.

Adsorption has proven to be an effective method of removing PFCs from contaminated water, and Yao et al. have shown the efficiency of PFOA removal using a variety of commercially available adsorbents, including granulated and powdered activated carbon, anion-exchange resin (AER), alumina, silica, and non-ion exchange polymers. AER has a very high adsorption constant of 200 $mg^{(1-n)}\ L^{n}\ g^{-1}$ compared to a value of 63 $mg^{(1-n)}\ L^{n}\ g^{-1}$ for granular activated carbon (GAC) [4]. Due to their hollow nanostructures that create high surface areas, carbon nanotubes have been effectively used as a PFC adsorbent, yet their practical application in PFC treatment is limited by available recycling technology [18]. Li et al. used multi-walled carbon nanotubes (MWCNs) to remove PFCs using electrochemical assistance by varying polarization potentials, and demonstrated some regeneration capabilities [18]. Polymeric membranes have also been used to reject PFOA from water using size exclusion and electrostatic forces. Boo et al. used negatively charged nanofiltration membranes in order to achieve approximately 90% PFOA rejection [13]. Patterson et al. used reverse osmosis (RO) membranes to reject PFOA and perfluorooctane sulfonate (PFOS) from drinking water [19]. The longevity of adsorbents has also been of interest; Du et al. used Fe_3O_4-loaded fluorinated vermiculite nanoparticles to selectively adsorb PFOS and regenerated the adsorbent using methanol for five cycles [20]. Despite such options, the regeneration ability of PFC adsorbent materials is limited. For example, activated carbon must undergo thermal regeneration in order to be reused.

The use of responsive polymeric materials provides an alternative opportunity to increase the efficiency of treating PFC contaminated water. Not only could they remove PFCs from water through adsorption mechanisms, but they could also controllably and reversibly desorb the PFCs by changing the environmental conditions. While the adsorption capacity of responsive polymeric materials may be lower than commonly used adsorbents such as activated carbon, the ease of recycling at low cost provides a benefit that makes them attractive pollutant adsorbents for the treatment of contaminated water. Poly-N-isopropylacrylamide (PNIPAm) has been widely studied as a lower critical solution temperature (LCST) polymer that exhibits a phase transition from a hydrophilic hydrated state to a dehydrated state at its LCST of 32 °C. By increasing the temperature, property changes in the polymer chains affect the hydrogen bonding of water molecules as the chains collapse in an aqueous environment [21]. PNIPAm exhibits one of the largest known volume phase transitions (VPTs) in response to environmental stimuli due to motion of the mobile water phase within the cross-linked polymer network [22]. Studies have shown that the hydrophobicity of PNIPAm can be controlled using slight temperature variations of a few degrees, thereby affecting adsorption of organic compounds [23]. Understanding of the mechanism behind PNIPAm's VPT has been limited and inconsistent until recently, with some asserting that the amide groups dehydrate first, while others state that the isopropyl groups dehydrate first and cause the chain to collapse [22, 24–27]. Wu et al., used non-resonance Raman temperature-jump spectrometry in order to determine that the hydrophobic isopropyl and methylene groups dehydrate much faster than the amide groups, and are thus responsible for initiating PNIPAm's VPT [22]. – Furthermore, the partitioning of nonpolar and polar solutes in both collapsed and swollen PNIPAm chains has been studied, with findings that nonpolar solutes tend to reside in the dryer regions of the polymer – [28]. The dehydration and rehydration of isopropyl groups on PNIPAm can therefore be leveraged for reversible adsorption of hydrophobic contaminants. Fig. 1 demonstrates the expected behavior of PNIPAm hydrogels as well as PNIPAm-functionalized membranes when the temperature is increased above its LCST of 32 °C. In an aqueous environment, PNIPAm hydrogels shrink at higher temperature. When functionalized within membrane pores, PNIPAm collapses at higher temperatures, increasing the apparent membrane pore size. The NIPAm concentration and PNIPAm degree of functionalization also have an impact. Increasing the NIPAm content in the polymerization mixture increases the polymer density when functionalized in membrane pores, thereby reducing permeance [29, 30].

Polyvinylidene fluoride (PVDF) membranes have been used as a base membrane for microfiltration and ultrafiltration processes due to their chemical resistance and mechanical stability [31–35]. Functionalizing PVDF membranes with responsive polymers gives the membrane new properties for advanced water separation. PVDF membranes have also been functionalized with PNIPAm to create temperature-responsive surfaces and pores [29, 30, 36]. When PNIPAm is formed inside PVDF membrane pores, controlling its hydrophobicity enables control over effective pore size, and therefore over water flux through the membrane. PNIPAm has been used to increase the adsorption of chlorinated organic compounds such as trichloroethylene (TCE) by raising the temperature just 3 degrees above the LCST [23].

In this paper, PNIPAm hydrogels and PNIPAm-functionalized PVDF membranes are used to adsorb and desorb PFOA using a temperature responsive behavior. The specific goals are: (1) to determine the adsorption isotherms of PFOA onto PNIPAm hydrogels, (2) to study the adsorption and desorption kinetics of PFOA onto PNIPAm hydrogels in water around PNIPAm's LCST using a pseudo-second order adsorption kinetics model, (3) to study the interaction properties between PNIPAm and PFOA versus PFOS in order to describe the relationship between interaction parameters of the functional groups involved in adsorption and desorption, and (4) to perform temperature swing adsorption using PNIPAm-functionalized PVDF membranes for continuous adsorption and desorption over multiples cycles.

2. Experimental

2.1. Materials

Full scale hydrophilized polyvinylidene fluoride 700 (PVDF-700) membranes were obtained from Nanostone Water, Inc., Oceanside, CA (average pore size: 250 nm, thickness: 0.172 mm, porosity: 0.4). All chemicals used were reagent grade. N-isopropylacrylamide (NIPAm) was purchased from VWR at 97% purity. N,N'-methylenebisacrylamide (BIS, 99%) and ammonium persulfate (APS, 98%) were received from Acros Organics. Ethanol (>99.9%), and methanol (>99.9%) were purchased form Sigma-Aldrich. Perfluorooctanoic acid (PFOA, 97%) was purchased from Alfa Aesar as Sodium perfluorooctanoate and Perfluorooctanesulfonic acid (PFOS, 98%) were obtained from Matrix Scientific as Potassium perfluorooctanesulfonate. Ultra-high purity (UHP) nitrogen gas was purchased from Scott Specialty Gases. Deionized ultra-filtered water (DIUF) was acquired from Fisher Scientific.

2.2. Synthesis of PNIPAm hydrogels

The PNIPAm hydrogels were prepared by temperature initiated free radical polymerization. First the DIUF was purged with UHP Nitrogen for 30 minutes because the presence of oxygen affects polymerization. The pre-polymerization mixture consisted of 30 g of NIPAm monomer in 200 mL of de-oxygenated DIUF, with 3 mol% BIS cross-linker and 2 mol% APS initiator for a molar ratio of NIPAm:BIS of 97:3.The solution was placed into petri dishes in a vacuum oven at 70 °C for two hours. The hydrogels were then removed from the plates, freeze dried, and crushed using a mortar and pastel. The broken up cross-linked PNIPAm hydrogels were then placed in deionized water to wash away any unreacted NIPAm monomer.

2.3. Synthesis of PNIPAm-functionalized PVDF membranes

PNIPAm monomer (6g, 13 wt%), BIS cross-linker (3 mol%), and APS initiator (2 mol%) were dissolved in de-oxygenated DIUF at room temperature to create the pre-polymerization mixture. The full-scale PVDF 700 membranes were developed in collaboration with Nanostone Sepro, Oceanside, CA. These hydrophilized membranes are supported by a backing fabric for increased stability, with a relatively open structure uniform geometry. The full-scale membrane sheets were cut into circles with diameters of 14 cm and were weighed prior to being mixed in the pre-polymerization mixture for 5 minutes. The pre-

polymerization mixture was then passed through the membrane at least 3 times using a vacuum pump in order to ensure the mixture was inside the membrane pores rather than only on the surface. The membrane surface was then dried using UHP nitrogen gas and placed between two glass plates and heated in an oven at 70 °C while being purged with UHP nitrogen for 2 hours. The PNIPAm-functionalized PVDF 700 membrane was then removed from the oven and washed with dilute ethanol to remove any unreacted monomer and stored in DIUF overnight. The membrane's mass increased an average of 15% post-functionalization. Fig. 2. is a schematic of the membrane functionalization process.

2.4. Characterization and analytical methods

2.4.1. Attenuated total reflectance Fourier transform infrared (ATR-FTIR)—

Attenuated total reflectance Fourier transform infrared (ATR-FTIR Varian 7000e) was used in order to confirm the presence of PNIPAm in the PVDF membrane. Samples of PNIPAm hydrogels as well as non-functionalized and PNIPAm-functionalized PVDF 700 membranes were analyzed to confirm successful polymerization of the blank PVDF membranes. PVDF membrane's CF_2 group's characteristic absorption band would be found at 1120–1280 cm^{-1} [30, 37]. NIPAm's –NH and –C=O groups' characteristic absorption bands would be found at 1540 cm^{-1} and 1650 cm^{-1}, respectively [30, 38–40]. The ATR-FTIR spectrum can be found in Fig. S1 in the supporting information.

2.4.2. Dynamic Light Scattering (DLS) for particle size—

Dynamic light scattering (DLS) was used in order to determine the apparent number average hydrodynamic diameter of the hydrogels, and the temperature was varied from 25 °C to 35 °C for 7 cycles to observe swelling behavior. The crosslinking density of the hydrogels was then increased and DLS was used to determine the average hydrodynamic diameter by raising the temperature above the LCST for 3 cycles. The swelling capacity was then compared to the less cross-linked hydrogel. Details of the DLS can be found in the supporting information.

2.4.3. Energy dispersive X-ray spectroscopy (EDS) analysis of PNIPAm hydrogels with PFOA—

After PFOA adsorption, PNIPAm hydrogel samples were dried and analyzed using energy dispersive X-ray spectroscopy (EDS, Oxford Instruments X-Max^N 80 detector). Hydrogel samples were freeze dried and mounted on the holder inside the scanning electron microscope chamber (FEI Helios Nanolab 660) and EDS analysis was performed in order to find the relative ratios of carbon, nitrogen, oxygen, and fluorine. Using the atomic ratios of fluorine, which only exists in PFOA, versus nitrogen, which only exists in PNIPAm, the adsorbed amount can be loosely predicted and compared to the equilibrium adsorption data.

2.4.4. Liquid Chromatography Mass Spectrometry (LC-MS/MS)—

All PFOA and PFOS samples were analyzed by liquid chromatography mass spectrometry (LC-MS/MS) separation. UPLC coupled electrospray ionization tandem mass spectrometry was used in this study. A bench top binary prominence Shimadzu chromatograph (Model: LC-20 AD) equipped with SIL 20 AC HT autosampler that was interfaced with an AB SCIEX Flash Quant mass spectrometer (MS/MS) (Model: 4000 Q TRAP). Limit of detections (LOD) for target analytes were 0.25 ng/L at S/N= 4. Seven calibration points with linear dynamic range

(LDR) were 2.5 – 320 ng/mL with R^2 values of 0.99968. Details of the LCMS method can be found in supporting information..

2.5. Temperature-responsive flux measurements

The PNIPAm-functionalized membrane was placed in a stirred cell acquired from Millipore in order to study its temperature responsive flux behavior. The cell was filled with DIUF and temperature was maintained using electrical heating tape. The cell had a digital thermocouple that enabled continuous monitoring of the temperature of the DIUF inside the cell. UHP nitrogen was used to pressurize the cell, which had a maximum pressure limit of 5.5 bars. Whenever the pressure was varied, water flux through the membrane was allowed to reach steady state before any samples were taken. When the temperature was varied, samples were only taken once the permeated water temperature was equal to the cell's internal temperature. Triplicate samples were taken to measure water flux by measuring permeated volume versus permeation time. Final runs were always conducted at conditions equal to the first run in order to test reversibility. Flux tests were performed using pure water at both 22 °C and at 35 °C with varying pressure in order to test the stability of the membrane, and can be found in the supporting information.. In order to further examine the temperature responsive nature of the PNIPAm functionalized membrane, the pressure was held constant and flux was measured as temperature was varied from 22 °C to 40 °C.

2.6. PFOA and PFOS equilibrium adsorption onto PNIPAm hydrogels

Adsorption of aqueous perfluorooctanoic acid (PFOA) using PNIPAm hydrogels was studied in order to determine the equilibrium adsorption values for aqueous PFOA-PNIPAm systems at near freezing (4°C), ambient (22°C), and above LCST (35°C) temperatures. Aqueous PFOA solutions (20 mL) were made using DIUF with concentrations ranging from 25 mg/L to 250 mg/L and adsorption was conducted using 0.5 g of PNIPAm hydrogels in each 20 mL vial. Three independent samples were analyzed for each concentration point, at each temperature. The details of the PNIPAm hydrogels and the analysis method can be found in the supporting information.. By plotting the equilibrium amount of PFOA adsorbed onto the hydrogels (q_e) versus the equilibrium PFAO concentration remaining in the aqueous phase (C_e), equilibrium adsorption curves can be experimentally determined for each isotherm.

The equilibrium adsorption isotherms of PFOA and PFOS were compared to calculated interaction parameter values. The different functional groups in the compounds yield different interaction parameters for the compounds. The apparent hydrogen bonding and dispersion interaction parameters of the various functional groups can be compared to the adsorption extent at temperatures above and below PNIPAm's LCST in order to explain relative adsorption behavior.

2.7. PFOA adsorption/desorption kinetics using PNIPAm hydrogels

The ability of PNIPAm particles to adsorb PFOA was studied as a function of time to determine the adsorption and desorption rates. Two grams of PNIPAm hydrogels were placed in 500 mL of water concentrated with 1000 ppm PFOA and shaken at 100 rpm in a temperature-controlled shaker set at 35 °C, with samples taken at various time intervals up to 24 hours. After reaching equilibrium, the hydrogels were removed from the aqueous PFOA

solution and placed in DIUF and shaken at 100 rpm at 20°C, with samples taken at various time intervals up to 18 hours. A sample volume of 1 mL was used in order to minimize the impact on the total solution concentration. Triplicate samples were always taken. Once taken, the sample was then analyzed using LCMS. Knowing the concentration of the aqueous phase at each point, the amount of adsorbed PFOA at each time interval was calculated by mass balance.

2.8. PFOA adsorption onto PNIPAm-functionalized PVDF membranes via convective flow

The PNIPAm-functionalized membrane was placed in a stirred cell acquired from Millipore in order to study its ability to adsorb and reversibly desorb PFOA as it is passed convectively through the membrane. In order to study adsorption, the cell was filled with 80 mL of DIUF concentrated with PFOA (0.5 mg/L) while the temperature was maintained at 35 °C using electrical heating tape. The cell had a digital thermocouple that enabled continuous monitoring of the temperature of the DIUF inside the cell. UHP nitrogen was used to pressurize the cell to 3.5 bar, yielding an average flux of 11 LMH. 80 mL of aqueous PFOA was passed through the membrane and the permeate was all collected in approximately 10 mL aliquots and PFOA concentrations were analyzed by LCMS using triplicate samples from each aliquot. Using mass balance, the amount of PFOA adsorbed in the membrane at each point could be calculated. Next, 80 mL of DIUF was placed in the cell at 22 °C with the pressure maintained at 3.5 bar in order to force the entire volume through the membrane to measure its desorption ability. Again, the entire permeate was collected in approximately 10 mL aliquots and the associated concentrations were analyzed using LCMS in order to determine the amount of desorbed PFOA. This adsorption/desorption study was repeated 5 times in order to test the longterm stability of the membrane and explore its ability for temperature swing adsorption.

3. Results and Discussion

Exploring PFOA adsorption onto PNIPAm hydrogels is important in order to determine the various adsorptive characteristics of the polymer prior to immobilizing it within membrane pores. Ultimately a functionalized membrane is needed for reversible adsorption over several cycles.

3.1. Swelling studies of PNIPAm hydrogels using dynamic light scattering

When the diameters of the 3 mol% crosslinked PNIPAm hydrogels were measured, the apparent hydrogel diameter decreased approximately by a factor of 10 when the temperature of the water was raised above its LCST. As shown in Fig. 3, the hydrogel diameter decreased from about 1000 nm to about 100 nm, indicating the successful polymerization and formation of the thermoresponsive PNIPAm hydrogels, and also indicating the repeatable thermoresponsive behavior of the hydrogels over several cycles. Adding a crosslinker is necessary for the stability of the hydrogels, and higher crosslinking density leads to more rigid particles [41]. Xiao et al. showed that even though 0.5 mol% BIS crosslinker enabled the greatest swelling change, a more stable polymer network was required to avoid the polymer chain being washed out when formed within membrane pores [30]. Wu et al. compared individual linear PNIPAm chains to corsslinked PNIPAm gels and found that

crosslinked gels have a higher transition temperature [42]. While Tanaka et al. claimed that chains located in loosely crosslinked domains deform significantly upon swelling compared to chains in densely crosslinked domains, Varga et al. showed that crosslinking density distribution within gels does not affect the VPT temperature, but rather only the system swelling capacity [43–45]. The crosslinking density of the PNIPAm hydrogels was varied in order to determine the effect on swelling capacity, which can be described as:

$$S = \frac{d_{swollen}}{d_{unswollen}} \quad (1)$$

Here, S represents the swelling capacity as the ratio of the apparent diameter of the hydrogels in the swollen state (25 °C) versus their apparent diameter in the un-swollen state (35 °C). The average swelling capacity was observed to be 10.3 for the hydrogels formed with 3 mol% crosslinker and 3.4 for the hydrogels formed with 10 mol% crosslinker, indicating that the swelling capacity of PNIPAm hydrogels is inversely related to crosslinking density. Furthermore, average diameter was larger for hydrogels made with higher cross-linking density in both swollen and collapsed states. The large standard deviation of hydrogel diameters in the swollen state can be attributed to the complexity of the chain entanglements, which will not always swell to the same extent.

3.2. Temperature responsive water flux through PNIPAm-functionalized PVDF 700 membranes

PNIPAm is known to exhibit a conformational change as temperature is raised above its LCST of 32 ºC. As temperature is increased, the isopropyl and methylene groups dehydrate, causing the backbone to collapse and causing the hydrophilic functional groups in the PNIPAm to release bound water and hydrogen bond with each other instead. When functionalized within membrane pores, the collapsing of PNIPAm chains at higher temperatures results in larger effective pore diameters. The linearity of the flux tests at constant temperature while varying pressure indicates membrane stability, and yielded fluxes of 1.6 LMH/bar at 22 °C and 28.8 LMH/bar at 35 °C, shown in Fig. S2 in supporting information.

3.2.1. Membrane Permeance aspects—Assuming laminar flow through uniform non-tortuous membrane pores and no slip at the wall, the Hagen-Poiseuille equation can be used to estimate relative pore diameters:

$$J_w = \frac{N\pi \Delta P}{A8\eta L}\left(\frac{D}{2}\right)^4 \quad (2)$$

Here, ΔP represents the pressure differential (3.5 bar), N represents the number of pores, A represents the area of permeation (45 cm^2), η represents viscosity of water, L represents the membrane thickness (0.172 mm), and D represents the pore diameter. The viscosity of water is adjusted for temperature over the temperature range. Number of pores and pore length are assumed to be constant, confirmed by measuring membrane thickness across the temperature range. The recorded water permeance values increased with temperature, displaying a

sharper increase of over 2-fold from between 28 ºC and 34 °C, shown in Fig. 4. The estimated relative effective pore diameters over the temperature range are also shown, demonstrating an increase of about 3.5-fold. This perceived coil-to-globule transition is explained by Oliveira et al., who show that the radius of gyration for PNIPAm decreases by a factor of about two when the temperature is raised above the LCST, but only when the number of monomer repeat units in the polymer chain is at least 32 [46].

3.3. PFOA equilibrium adsorption onto PNIPAm hydrogels

Adsorption of PFOA onto PNIPAm hydrogels was evaluated at various PFOA concentrations for three different temperatures. Due to relatively low water solubility, PFOA concentrations were varied between 25 and 250 ppm. For this low concentration range, the adsorption isotherms can be fitted using a Freundlich isotherm equation, which empirically describes adsorption of solutes from a liquid onto a solid.

$$q_e = K_d C_e^{1/n} \tag{3}$$

Here, q_e (mg/g) represents the amount of solute (PFOA) adsorbed per unit weight of solid (PNIPAm) at equilibrium, in units of mg/g, while c_e (mg/L) represents the equilibrium concentration of solute in solution (water) when the adsorbed amount is equal to q_e, and k_d (L/g) is the distribution coefficient, and n is the correction factor. While, the Freundlich isotherm does not predict that adsorption maximum, this experiment explores the linear part of the isotherm.

The observed isotherms fit the experimental data well, as shown in Fig. 5A. The k_d values increased significantly as temperature was raised, with a larger jump between 20 °C and 35 °C due to the polymer's LCST value of 32 °C. Freundlich adsorption isotherms for PFOA on PNIPAm gels yields K_d values of 0.073 L/g at 35 °C, 0.026 L/g at 22 °C, and 0.007 L/g at 4 °C. As temperature is increased, the isopropyl groups of the PNIPAm particles dehydrate fast, and increase adsorption of PFOA due to its hydrophobic tail. This behavior, where hydrophobic contaminants will partition into the more dehydrated parts of the polymer, is shown in Figure 5B.

The large increase in hydrogel adsorption capacity of PFOA from 4 °C to 22 °C cannot be attributed to the LCST conformational change of PNIPAm and therefore requires another explanation. Futscher et al. studied the conformational changes of PNIPAm versus its NIPAm monomer using Fourier transform infrared spectroscopy to probe changes, and found that NIPAm exhibits a nearly linear change with temperature compared to PNIPAm, which displays a discontinuous shift across the LCST [47]. The presence of NIPAm in the hydrogels is a reasonable explanation for the difference. Xiao et al. demonstrated decreased partitioning of hydrophilic orange II onto PNIPAm hydrogels by raising temperature. There was a significant change in partitioning when temperature was raised in the region below PNIPAm's LCST [23]. PFOA however is structured like a surfactant with a long hydrophobic tail and a hydrophilic carboxylic head, leading to interaction with both the hydrophobic and hydrophilic functional groups of PNIPAm. Another explanation could be the effect of temperature on ionization, where increasing temperature increases Ka and

decreases pKa, thereby increasing ionization in weak acids. The counter ion for PFOA in these experiments is Na^+, which has been shown to interact with the amide group of PNIPAm, showing greater interaction at higher temperatures [48].

3.4. PFOA adsorption/desorption kinetics using PNIPAm hydrogels

In order to further understand and model the adsorption kinetics, a pseudo-second order (PSO) model that has been used to explain sorption rate whereby adsorption capacity is proportional to sorbent active sites occupied was used [49].

$$\frac{\partial q_t}{\partial t} = k_2(q_e - q_t)^2 \tag{4}$$

Here, q_t and q_e (mg/g) represent the amount of PFOA adsorbed at time, t (hrs), and at equilibrium respectively, while k_2 is the second order adsorption rate constant and $\vartheta 0$ is the initial adsorption rate (mg/g/h). By integrating from time 0 to time t, equation 4 can be rearranged as follows:

$$\frac{t}{q_t} = \frac{1}{k_2 q_e^2} + \frac{t}{q_e} = \frac{1}{\vartheta_0} + \frac{t}{q_e} \tag{5}$$

By plotting t/q_t vs. t, a linear fit enables the determination of q_e and k_2 values for both adsorption and desorption, as shown in Table 1 along with R^2 values. These plots are shown in Fig. S3. Kinetic adsorption and desorption values were calculated, and then used to calculate adsorption and desorption data points to compare with the experimental data, which are shown in Fig. 6. Over half of the adsorbed amount adsorbs in the first hour, and over half of the desorbed amount desorbs within the first hour, as shown in Fig. 6B. There is no longer any appreciable adsorption or desorption after 15 hours.

Here, the q_e values can be compared to the equilibrium isotherm experimental data for consistency, and fall within 20% of the predicted value from the adsorption isotherms. The initial desorption rate was greater than the initial adsorption rate, both in the same range as PFOA adsorption onto GAC, reported as 16.2 mg/g/h [4], even though the distribution coefficients are lower.

3.5. EDS analysis of PNIPAm hydrogels with adsorbed PFOA

The molar ratio of Nitrogen (N) to Fluorine (F) is a good indicator of the amount of PFOA adsorbed, since Nitrogen is only present in the PNIPAm hydrogel and Fluorine is only present in the PFOA molecules. The approximate molar ratio of N:F is 52:1, and since there is 1 N present per PNIPAm monomer, and 15 F present per PFOA molecule, the molar ratio of PNIPAm monomers in the hydrogel to PFOA molecules can be approximated as 780:1, yielding an estimated 4.7 mg/g adsorbed. In the experimental equilibrium adsorption data found in Table 2, the amount adsorbed for that hydrogel was 3.5 mg/g, which is on the same order of magnitude. This analysis confirms the presence and adsorption of PFOA onto the PNIPAm hydrogels, but should not be used as a quantitative tool because of the high standard deviation of values between the three different sites of the sample. Table S1 in the

supporting information shows full EDS analysis results of three different sample sites. The standard deviation for F content is 0.37 for the three sites, indicating that F is not evenly distributed throughout the hydrogel.

3.6. Adsorption of PFOA and PFOS onto PNIPAm hydrogels using interaction parameters

The adsorption of contaminants such as PFOA and PFOS onto PNIPAm in an aqueous environment can be explained using interaction parameters. When the temperature is below PNIPAm's LCST, the polymer swells with bound water (to its hydrophilic amide functional groups) and bulk water [47]. Therefore, the adsorption of PFOA and PFOS onto the hydrogel will can be partly explained by the difference between 1) the hydrogen bonding interaction (δ_h) between the polymer's hydrophilic functional group and the hydrophilic groups of PFOA and PFOS (carboxylic and sulfonate groups respectively) and 2) the hydrogen bonding interaction (δ_h) between the hydrophilic functional groups of PFOA and PFOS and the water. As temperature is raised and the isopropyl groups dehydrate to initiate chain collapse, adsorption can be partly explained by the difference between 1) the dispersion interaction (δ_d) between the hydrophobic functional groups of PNIPAm (isopropyl) and of the target perfluorinated compound (fluorinated carbon tail) and 2) the hydrogen bonding interaction (δ_h) between the hydrophilic functional groups of PFOA and PFOS (carboxylic and sulfonate groups respectively) and the water. The difference occurs because the amide groups in PNIPAm will release the bound water and interact with other PNIPAm amide groups following chain collapse. Any ionization effects on interaction are not considered here. These basic interactions between the aqueous environment, PFOA, and PNIPAm hydrogels are depicted in Fig. 7

The effective interaction parameters for various compounds can be calculated using a group contribution method developed by Hansen and Beerbower [50]. Barton found that it is convenient and reliable to use structural combination methods to estimate interaction parameters, and assumes additive cohesion parameter components for groups present in a molecule [50]. The reported group contribution values of molar attraction constants, molar volumes, and molar cohesive energy can be found in Table S2 in supporting information, while calculated values for solubility parameter values of interest can be found in Tables S3 and S4 in supporting information, as well as reference values of compounds with similar structures [51].

In order to compare the impact of these described interaction parameters on adsorption capacity, adsorption of PFOA and PFOS was compared. The hydrophobic fluorinated tail of both PFOA and PFOS are the same, and the dispersion interaction parameter associated with the tail is predicted to be around 20.8 $MPa^{1/2}$. However, the hydrophilic head groups of the two molecules differ. PFOA has a carboxylic group, which has a hydrogen bonding interaction parameter of 13.2 $MPa^{1/2}$ while PFOS has a sulfonate group, which has a higher hydrogen bonding interaction parameter. Sulfonic groups' affinity to form hydrogen bonds with OH groups has been shown to increase the interaction of compounds with polar solvents upon sulfonation [52, 53]. Therefore, it would be expected that PFOS would partition less into the PNIPAm hydrogels than PFOA because of the stronger hydrogen bonding interaction between its sulfonate head group and the surrounding aqueous

environment. The lack of measured cohesive energy density (CED) values for sulfonated polymers causes uncertainty in using group contribution calculations to determine interaction parameters [52]. Adsorption isotherm data for PFOS can be found in Fig. S4, with K_d values for PFOA and PFOS are detailed in Table 3. The ratio of K_d values for PFOS adsorption at 35 °C versus 20 °C is only 1.1, compared to a much larger ratio of 2.8 for PFOA. While equilibrium adsorption of PFOS by PNIPAm is higher than adsorption of PFOA below the LCST, much like PFOS adsorption onto GAC and other adsorbents, it is much lower above the LCST due to the presence of the sulfonate group [2–4]. Therefore, conducting temperature swing adsorption of PFOS using PNIPAm would not provide any new information.

3.7. Predicting aqueous PFOA solution concentrations:

Using the adsorption isotherm values, the potential to concentrate aqueous PFOA solutions can be examined. Given an initial aqueous PFOA concentration, the equilibrium adsorption isotherm can be used to determine the extent of adsorption by computing q_e and C_e from equations 7 and 8:

$$q_e = K_d C_e^{1/n} \tag{7}$$

$$C_i V_w = q_e m_h + C_e V_W \tag{8}$$

Equation 7 represents the adsorption isotherms. In equation 8, C_i is the initial aqueous PFOA concentration, V_w is the total water volume, and m_h is the hydrogel mass. Equation 7 can be combined with equation 8 in order to determine both C_e and q_e values if the other values (V_w, m_h, C_i) are known, and then equation 5 can be used to find q_t versus t values in order to predict adsorption versus time data.

Assuming 1g of PNIPAm hydrogels were placed in 20 mL of 20 mg/L aqueous PFOA and allowed to reach equilibrium at 35 °C, the K_d values indicate that 0.31 mg/g would be adsorbed, resulting in a final equilibrium concentration of 4.3 mg/L. Assuming the PNIPAm hydrogels with adsorbed PFOA are then removed and placed in 3 mL of pure water at 22 °C, the K_d values would indicate that 0.28 mg/g would remain adsorbed, resulting in a final equilibrium concentration of 11 mg/L. The final equilibrium concentration achieved was 10 mg/L, agreeing with the adsorption isotherm experiments in Fig. 5.

3.8. Membrane Adsorption/Desorption:

PNIPAm-functionalized membrane adsorption and desorption of PFOA is plotted in Fig. 8. Using the hydrogel equilibrium isotherms, a value of 0.5 mg/L for C_e would yield q_e values of 0.04 mg/g for the PFOA adsorption isotherm. The upper limit of functionalized membrane adsorption of PFOA is on the same order of magnitude. Desorption was conducted with pure DIUF water at 20 °C. After 300 mL of pure DIUF water was permeated, 80% of previously adsorbed PFOA was desorbed. The initial rates were calculated in terms of mg PFOA adsorbed/L of solution permeated. The initial adsorption rate was 0.14 mg/L, while the initial desorption rate was 0.17 mg/L. It was shown that after

80 mL of permeated solution (aqueous 0.5 mg/L PFOA for adsorption and pure DIUF for desorption), both adsorption and desorption rates were much lower. Therefore, for conducting temperature swing adsorption studies, only 80 mL was used for each adsorption and desorption cycle.

Temperature swing adsorption was conducted over 5 cycles, shown in Fig. 9. About 0.01 mg of PFOA was adsorbed after 80 mL of 0.5 mg/L of aqueous PFOA was permeated through the membrane at 3.5 bar and 35 °C, meaning that about 25% of the 0.04 mg of permeated PFOA was adsorbed. Residence time would have an impact on membrane adsorption performance, but this paper focuses on the ability to regenerate the membrane and perform temperature swing adsorption. When 80 mL of pure water was passed through the membrane at the same pressure of 3.5 bar, at a temperature of 20 °C, about 60% of the adsorbed PFOA was desorbed. For the next 4 cycles, adsorption capacity seemed to be constant after passing 80 mL of aqueous PFOA through the 596 membrane at the same 3.5 bar pressure. Also, desorption was relatively constant at between 50–60% of the adsorbed amount. After the first adsorption/desorption cycle, however, more than 90% of the PFOA adsorbed in consequent adsorption cycle was desorbed in each following desorption cycle, indicating promise for the use of PNIPAm-functionalized membranes for temperature swing adsorption. While the pressure was held constant, the flux was maintained throughout each cycle with little deviation. Every time the temperature was raised to 35 °C for adsorption, the flux was around 10.6 LMH, while the flux dropped to around 1.2 LMH when the temperature was dropped to 20 °C, with standard deviations of 0.5 LMH and 0.1 LMH, respectively. The ability to quickly and easily desorb contaminant from the functionalized membrane is encouraging for use as an adsorbent with greater regeneration ability than other adsorbents.

In order to confirm that desorption using pure water must be conducted below LCST, two adsorption/desorption cycles were conducted using 0.5mg/L aqueous PFOA for each adsorption cycle and pure DIUF for each desorption cycle, shown in Fig. 10. In both cases, adsorption was conducted above PNIPAm's LCST, while the first desorption cycle was conducted below PNIPAm's LCST. However, for the second desorption cycle, pure DIUF at 35 °C was used rather than at 20 °C to prove that desorption is insignificant if T > LCST. For the first cycle, 0.016 mg of PFOA was adsorbed, followed by about 60% desorption using pure water at 20 °C. A second adsorption cycle yielded the same adsorption capacity as the first cycle. However, only 13% of adsorbed PFOA was desorbed using water above LCST, compared to 60% with 20 °C water, thereby proving that LCST behavior plays a role in enhancing desorption. In the control run, where PFOA was permeated through a blank PVDF membrane, less than 1% was adsorbed, indicating that adsorption takes place in the polymeric PNIPAm domain. Flux above LCST was constant at 37 LMH, while flux below LCST was 2.5 LMH. Pressure was set at 2.75 bar because the functionalized membrane used was not as tight as the one used for the temperature swing adsorption cycles.

4. Conclusion:

The reversible swelling behavior of PNIPAm, in hydrogel form and within membrane pores, is confirmed for use as a temperature swing adsorbent. Even though the Freundlich

distribution coefficient of 0.007 L/g for PFOA is less than other adsorbent materials, the initial PFOA adsorption rate of 28 mg/g/h onto PNIPAm hydrogels is comparable to published PFOA adsorption rates using other adsorbents such as GAC. The ability to then desorb PFOA at an even higher initial rate than adsorption, and recycle the PNIPAm cost effectively when immobilized in PVDF membrane pores, makes PNIPAm and the use of stimuli responsive polymeric materials a new and attractive avenue for the reversible adsorption and treatment of PFCs. Temperature swing adsorption was conducted over 5 cycles, where 60% of the PFOA adsorbed in the first cycle was desorbed, followed by desorption of over 90% of the PFOA adsorbed in the subsequent cycles. Regeneration of adsorbents for PFCs is an area that requires advancement, and temperature swing adsorption using stimuli responsive membranes is a promising avenue for research. The apparent interaction parameters of functional groups were calculated and used to estimate the relative adsorption of PFOA and PFOS, demonstrating that varying the interaction parameters of functional groups on contaminants can have a large impact on an ability to perform temperature swing adsorption. Stimuli-responsive, functionalized polymeric membranes for reversible contaminant adsorption with high initial rates provide a very exciting technology for the possible removal of toxic organic contaminants removal from water.

Symbols and Nomenclature

Symbol	Description
q_e (mg/g)	Adsorption at equilibrium
q_t (mg/g)	Adsorption at time, t
$\frac{q_{2,1}(T > LCST)}{q_{2,1}(T < LCST)}$	Ratio of adsorption of compound 1 (PFOA/PFOS) onto compound 2 (water) above LCST to adsorption of compound 2 onto compound 2 below LCST
C_i (mg/L)	Initial concentration
C_e (mg/L)	Equilibrium concentration
K_d (L/g)	Freundlich distribution coefficient
k_2	Second order adsorption/desorption rate constant
ϑ_0 (mg/g/h)	Initial rate of adsorption/desorption
V_w (mL)	Water volume
m_h (g)	Hydrogel mass
$\delta_{d,1}$	Dispersion interaction parameter for compound 1 (PNIPAm)
$\delta_{d,2}$	Dispersion interaction parameter for compound 2 (PFOA/PFOS)
$\delta_{d,3}$	Dispersion interaction parameter for compound 3 (Water)
$\delta_{h,1}$	Hydrogen bonding interaction parameter for compound 1
$\delta_{h,2}$	Hydrogen bonding interaction parameter for compound 2
$\delta_{h,3}$	Hydrogen bonding interaction parameter for compound 3

Supplementary Material

Refer to Web version on PubMed Central for supplementary material.

Acknowledgements:

This research is supported by the NIH-NIEHS-SRC (Award number: P42ES007380) and the NSF KY EPSCoR grant (Grant no: 1355438). LC-MS analysis was supported by UK-CARES through Grant P30 ES026529. Its contents are solely the responsibility of the authors and do not necessarily represent the official views of the NIEHS.

References:

[1]. Lundquist N, Sweetman MJ, Scroggie K, Worthington M, Esdaile L, Alboaiji S, Plush SE, Hayball JD, Chalker JM, Polymer supported carbon for safe and effective remediation of PFOA-and PFOS-contaminated water, ACS Sustainable Chemistry & Engineering, (2019) 11044–11049.

[2]. Zhou Q, Deng S, Zhang Q, Fan Q, Huang J, Yu G, Sorption of perfluorooctane sulfonate and perfluorooctanoate on activated sludge, Chemosphere, 81 (2010) 453458.

[3]. Du Z, Deng S, Zhang S, Wang B, Huang J, Wang Y, Yu G, Xing B, Selective and High Sorption of Perfluorooctanesulfonate and Perfluorooctanoate by Fluorinated Alkyl Chain Modified Montmorillonite, The Journal of Physical Chemistry C, 120 (2016) 16782–16790.

[4]. Yao Y, Volchek K, Brown CE, Robinson A, Obal T, Comparative study on adsorption of perfluorooctane sulfonate (PFOS) and perfluorooctanoate (PFOA) by different adsorbents in water, Water Science and Technology, 70 (2014) 1983–1991. [PubMed: 25521134]

[5]. Schultz MM, Barofsky DF, Field JA, Quantitative Determination of Fluorotelomer Sulfonates in Groundwater by LC MS/MS, Environmental Science & Technology, 38 (2004) 1828–1835. [PubMed: 15074696]

[6]. Murakami M, Shinohara H, Takada H, Evaluation of wastewater and street runoff as sources of perfluorinated surfactants (PFSs), Chemosphere, 74 (2009) 487–493. [PubMed: 19054542]

[7]. Tang CY, Fu QS, Robertson AP, Criddle CS, Leckie JO, Use of Reverse Osmosis Membranes to Remove Perfluorooctane Sulfonate (PFOS) from Semiconductor Wastewater, Environmental Science & Technology, 40 (2006) 7343–7349. [PubMed: 17180987]

[8]. Vecitis CD, Park H, Cheng J, Mader BT, Hoffmann MR, Treatment technologies for aqueous perfluorooctanesulfonate (PFOS) and perfluorooctanoate (PFOA), Frontiers of Environmental Science & Engineering in China, 3 (2009) 129–151.

[9]. Liou JSC, Szostek B, DeRito CM, Madsen EL, Investigating the biodegradability of perfluorooctanoic acid, Chemosphere, 80 (2010) 176–183. [PubMed: 20363490]

[10]. Zhang L.-h., Cheng J.-h., You X, Liang X.-y., Hu Y.-y., Photochemical defluorination of aqueous perfluorooctanoic acid (PFOA) by Fe 0/GAC microelectrolysis and VUV-Fenton photolysis, Environmental Science and Pollution Research, 23 (2016) 13531–13542.

[11]. Yang S, Cheng J, Sun J, Hu Y, Liang X, Defluorination of Aqueous Perfluorooctanesulfonate by Activated Persulfate Oxidation, PLoS ONE, 8 (2013) 110.

[12]. Park H, Vecitis CD, Cheng J, Choi W, Mader BT, Hoffmann MR, Reductive Defluorination of Aqueous Perfluorinated Alkyl Surfactants: Effects of Ionic Headgroup and Chain Length, The Journal of Physical Chemistry A, 113 (2009) 690696.

[13]. Boo C, Wang Y, Zucker I, Choo Y, Osuji CO, Elimelech M, High Performance Nanofiltration Membrane for Effective Removal of Perfluoroalkyl Substances at High Water Recovery, Environmental Science & Technology, 52 (2018) 7279–7288. [PubMed: 29851340]

[14]. Senevirathna STMLD, Tanaka S, Fujii S, Kunacheva C, Harada H, Shivakoti BR, Okamoto R, A comparative study of adsorption of perfluorooctane sulfonate (PFOS) onto granular activated carbon, ion-exchange polymers and nonion-exchange polymers, Chemosphere, 80 (2010) 647–651. [PubMed: 20546842]

[15]. Du Z, Deng S, Bei Y, Huang Q, Wang B, Huang J, Yu G, Adsorption behavior and mechanism of perfluorinated compounds on various adsorbents—A review, Journal of Hazardous Materials, 274 (2014) 443–454. [PubMed: 24813664]

[16]. Senevirathna STMLD, Tanaka S, Fujii S, Kunacheva C, Harada H, Ariyadasa BHAKT, Shivakoti BR, Adsorption of perfluorooctane sulfonate (n-PFOS) onto non ion-exchange polymers and granular activated carbon: Batch and column test, Desalination, 260 (2010) 29–33.

[17]. Chen X, Xia X, Wang X, Qiao J, Chen H, A comparative study on sorption of perfluorooctane sulfonate (PFOS) by chars, ash and carbon nanotubes, Chemosphere, 83 (2011) 1313–1319. [PubMed: 21531440]

[18]. Li X, Chen S, Quan X, Zhang Y, Enhanced Adsorption of PFOA and PFOS on Multiwalled Carbon Nanotubes under Electrochemical Assistance, Environmental Science & Technology, 45 (2011) 8498–8505. [PubMed: 21861476]

[19]. Patterson C, Burkhardt J, Schupp D, Krishnan ER, Dyment S, Merritt S, Zintek L, Kleinmaier D, Effectiveness of point-of-use/point-of-entry systems to remove per- and polyfluoroalkyl substances from drinking water, AWWA Water Science, 1 (2019) e1131.

[20]. Du Z, Deng S, Zhang S, Wang W, Wang B, Huang J, Wang Y, Yu G, Xing B, Selective and Fast Adsorption of Perfluorooctanesulfonate from Wastewater by Magnetic Fluorinated Vermiculite, Environmental Science & Technology, 51 (2017) 8027–8035. [PubMed: 28614945]

[21]. Yim H, Kent MS, Mendez S, Balamurugan SS, Balamurugan S, Lopez GP, Satija S, Temperature-dependent conformational change of PNIPAM grafted chains at high surface density in water, Macromolecules, 37 (2004) 1994–1997.

[22]. Wu T-Y, Zrimsek AB, Bykov SV, Jakubek RS, Asher SA, Hydrophobic Collapse Initiates the Poly(N-isopropylacrylamide) Volume Phase Transition Reaction Coordinate, The Journal of Physical Chemistry B, 122 (2018) 3008–3014. [PubMed: 29481081]

[23]. Xiao L, Isner AB, Hilt JZ, Bhattacharyya D, Temperature responsive hydrogel with reactive nanoparticles, J Appl Polym Sci, 128 (2013) 1804–1814. [PubMed: 30518988]

[24]. Lai H, Wu P, A infrared spectroscopic study on the mechanism of temperatureinduced phase transition of concentrated aqueous solutions of poly (Nisopropylacrylamide) and N-isopropylpropionamide, Polymer, 51 (2010) 1404–1412.

[25]. Ramon O, Kesselman E, Berkovici R, Cohen Y, Paz Y, Attenuated total reflectance/fourier transform infrared studies on the phase-separation process of aqueous solutions of poly (n-isopropylacrylamide), Journal of Polymer Science Part B: Polymer Physics, 39 (2001) 1665–1677.

[26]. Sun S, Hu J, Tang H, Wu P, Chain collapse and revival thermodynamics of poly (N-isopropylacrylamide) hydrogel, The Journal of Physical Chemistry B, 114 (2010) 9761–9770. [PubMed: 20666519]

[27]. Sun B, Lin Y, Wu P, Siesler HW, A FTIR and 2D-IR spectroscopic study on the microdynamics phase separation mechanism of the poly (N-isopropylacrylamide) aqueous solution, Macromolecules, 41 (2008) 1512–1520.

[28]. Kanduč M, Kim WK, Roa R, Dzubiella J, Transfer Free Energies and Partitioning of Small Molecules in Collapsed PNIPAM Polymers, The Journal of Physical Chemistry B, (2018) 720–728.

[29]. Xiao L, Davenport DM, Ormsbee L, Bhattacharyya D, Polymerization and Functionalization of Membrane Pores for Water Related Applications, Ind Eng Chem Res, 54 (2015) 4174–4182. [PubMed: 26074669]

[30]. Xiao L, Isner A, Waldrop K, Saad A, Takigawa D, Bhattacharyya D, Development of Bench and Full-Scale Temperature and pH Responsive Functionalized PVDF Membranes with Tunable Properties, J Memb Sci, 457 (2014) 39–49. [PubMed: 24944434]

[31]. Gui M, Ormsbee LE, Bhattacharyya D, Reactive Functionalized Membranes for Polychlorinated Biphenyl Degradation, Industrial & Engineering Chemistry Research, 52 (2013) 10430–10440.

[32]. Smuleac V, Bachas L, Bhattacharyya D, Aqueous-phase synthesis of PAA in PVDF membrane pores for nanoparticle synthesis and dichlorobiphenyl degradation, Journal of Membrane Science, 346 (2010) 310–317. [PubMed: 20161475]

[33]. Lewis SR, Datta S, Gui M, Coker EL, Huggins FE, Daunert S, Bachas L, Bhattacharyya D, Reactive nanostructured membranes for water purification, Proceedings of the National Academy of Sciences, 108 (2011) 8577–8582.

[34]. Xu J, Bhattacharyya D, Fe/Pd Nanoparticle Immobilization in Microfiltration Membrane Pores: Synthesis, Characterization, and Application in the Dechlorination of Polychlorinated Biphenyls, Industrial & Engineering Chemistry Research, 46 (2007) 2348–2359.

[35]. Islam MS, Hernández S, Wan H, Ormsbee L, Bhattacharyya D, Role of membrane pore polymerization conditions for pH responsive behavior, catalytic metal nanoparticle synthesis, and PCB degradation, Journal of Membrane Science, 555 (2018) 348–361. [PubMed: 30718939]

[36]. Bera A, Kumar CU, Parui P, Jewrajka SK, Stimuli responsive and low fouling ultrafiltration membranes from blends of polyvinylidene fluoride and designed library of amphiphilic poly(methyl methacrylate) containing copolymers, Journal of Membrane Science, 481 (2015) 137–147.

[37]. Ying L, Yu WH, Kang ET, Neoh KG, Functional and Surface-Active Membranes from Poly(vinylidene fluoride)-graft-Poly(acrylic acid) Prepared via RAFT-Mediated Graft Copolymerization, Langmuir, 20 (2004) 6032–6040. [PubMed: 16459627]

[38]. Li Y, Chu L-Y, Zhu J-H, Wang H-D, Xia S-L, Chen W-M, Thermoresponsive Gating Characteristics of Poly(N-isopropylacrylamide)-Grafted Porous Poly(vinylidene fluoride) Membranes, Industrial & Engineering Chemistry Research, 43 (2004) 2643–2649.

[39]. Yu J-Z, Zhu L-P, Zhu B-K, Xu Y-Y, Poly(N-isopropylacrylamide) grafted poly(vinylidene fluoride) copolymers for temperature-sensitive membranes, Journal of Membrane Science, 366 (2011) 176–183.

[40]. Ying L, Kang ET, Neoh KG, Synthesis and Characterization of Poly(Nisopropylacrylamide)-graft-Poly(vinylidene fluoride) Copolymers and Temperature-Sensitive Membranes, Langmuir, 18 (2002) 6416–6423.

[41]. Boon N, Schurtenberger P, Swelling of micro-hydrogels with a crosslinker gradient, Physical Chemistry Chemical Physics, 19 (2017) 23740–23746.

[42]. Wu C, Zhou S, Au-yeung SCF, Jiang S, Volume phase transition of spherical microgel particles, Die Angewandte Makromolekulare Chemie, 240 (1996) 123–136.

[43]. Tanaka T, Fillmore DJ, Kinetics of swelling of gels, The Journal of Chemical Physics, 70 (1979) 1214–1218.

[44]. Acciaro R, Gilányi T, Varga I, Preparation of Monodisperse Poly(Nisopropylacrylamide) Microgel Particles with Homogenous Cross-Link Density Distribution, Langmuir, 27 (2011) 7917–7925. [PubMed: 21591700]

[45]. Su W, Zhao K, Wei J, Ngai T, Dielectric relaxations of poly(Nisopropylacrylamide) microgels near the volume phase transition temperature: impact of cross-linking density distribution on the volume phase transition, Soft Matter, 10 (2014) 8711–8723. [PubMed: 25263641]

[46]. de Oliveira TE, Marques CM, Netz PA, Molecular dynamics study of the LCST transition in aqueous poly(N-n-propylacrylamide), Physical Chemistry Chemical Physics, 20 (2018) 10100–10107.

[47]. Futscher MH, Philipp M, Müller-Buschbaum P, Schulte A, The role of backbone hydration of poly (N-isopropyl acrylamide) across the volume phase transition compared to its monomer, Scientific reports, 7 (2017) 17012.

[48]. Du H, Qian X, Molecular dynamics simulations of PNIPAM-co-PEGMA copolymer hydrophilic to hydrophobic transition in NaCl solution, Journal of Polymer Science Part B: Polymer Physics, 49 (2011) 1112–1122.

[49]. Ho YS, McKay G, Pseudo-second order model for sorption processes, Process Biochemistry, 34 (1999) 451–465.

[50]. Barton AFM, Handbook of Solubility Parameters and Other Cohesion Parameters 2nd Edition ed, CRC Press, Inc, Boca Raton, Florida, 1991.

[51]. Hansen CM, Hansen Solubility Parameters: A User's Handbook, CRC Press, 2002.

[52]. Ferrell WH, Kushner DI, Hickner MA, Investigation of polymer–solvent interactions in poly(styrene sulfonate) thin films, Journal of Polymer Science Part B: Polymer Physics, 55 (2017) 1365–1372.

[53]. Gong C, Guan R, Shu Y-C, Chuang F-S, Tsen W-C, Effect of sulfonic group on solubility parameters and solubility behavior of poly(2,6-dimethyl-1,4-phenylene oxide), Polymers for Advanced Technologies, 18 (2007) 44–49.

Highlights:

- PNIPAm is successfully polymerized in PVDF membrane pores via pore filling method
- Reversible PNIPAm swelling in membrane pores is verified as a function of temperature
- PNIPAm thermo-responsively adsorbs PFOA when T > LCST
- Interaction parameters are used to describe relative adsorption
- PNIPAm-functionalized PVDF membranes can be reused for PFOA adsorption

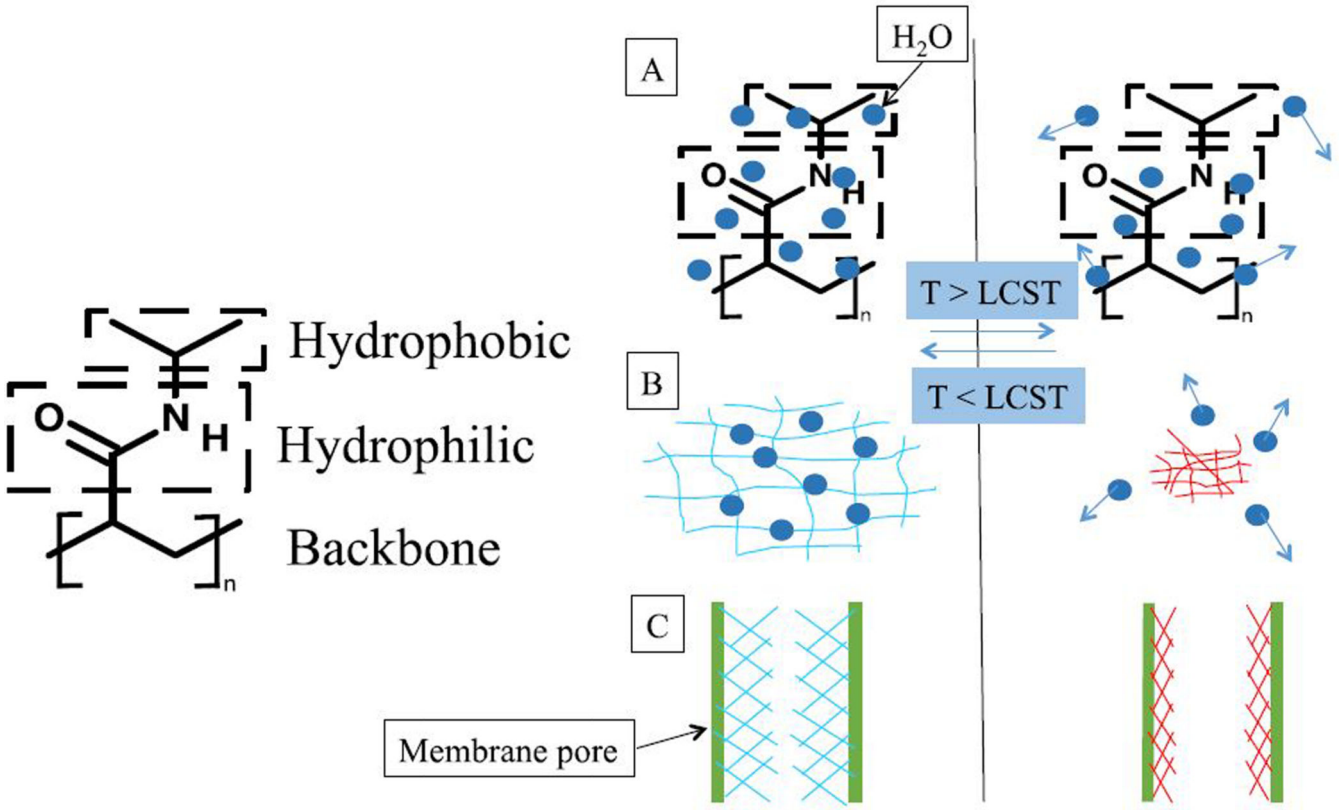

Figure 1:
Schematic of thermo-responsive behavior of PNIPAm hydrogels and PNIPAmfunctionalized membranes in aqueous environment: (A) isopropyl groups followed by polymer backbone are the first to dehydrate when temperature is raised above LCST (B) PNIPAm hydrogels swell and expand in aqueous environment below LCST (C) effective pore opening of a PNIPAm-functionalized membrane is larger when the polymer is in the collapsed state above its LCST.

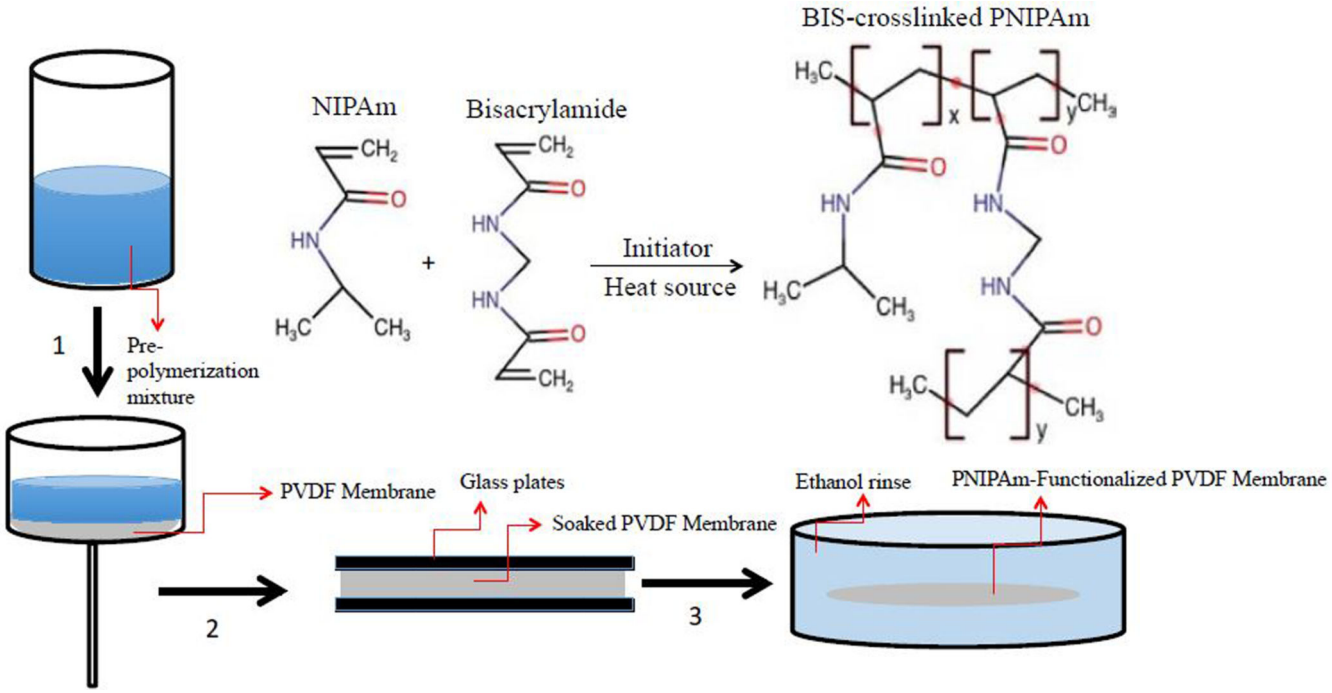

Figure 2:

Schematic of the membrane functionalization process. In step 1, the pre-polymerization mixture is passed through the PVDF membrane in order to wet the pores. In step 2, the soaked membrane is placed between two glass plates and heated at 70 ºC for two hours. In step 3, the functionalized membrane is washed in ethanol to remove unreacted monomer.

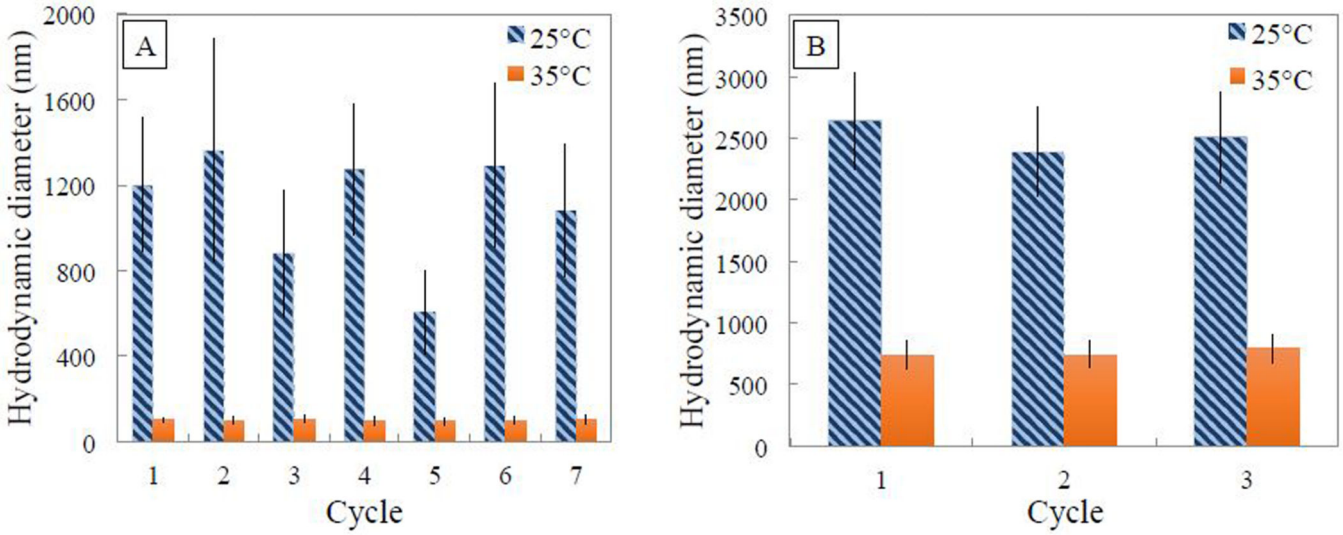

Figure 3:

(A) Hydrodynamic diameter (number average) of PNIPAm hydrogels (13 wt% NIPAm, 3mol% Bisacrylamide crosslinker, 2 mol% APS initiator) in aqueous solution measured using DLS changing the solution temperature from 25 °C to 35 °C over seven cycles. (B) Hydrodynamic diameter (number average) of PNIPAm hydrogels (13 wt% NIPAm, 10 mol % Bisacrylamide crosslinker, 2 mol% APS initiator) in aqueous solution measured using DLS changing the solution temperature from 25 °C to 35 °C, over three cycles.

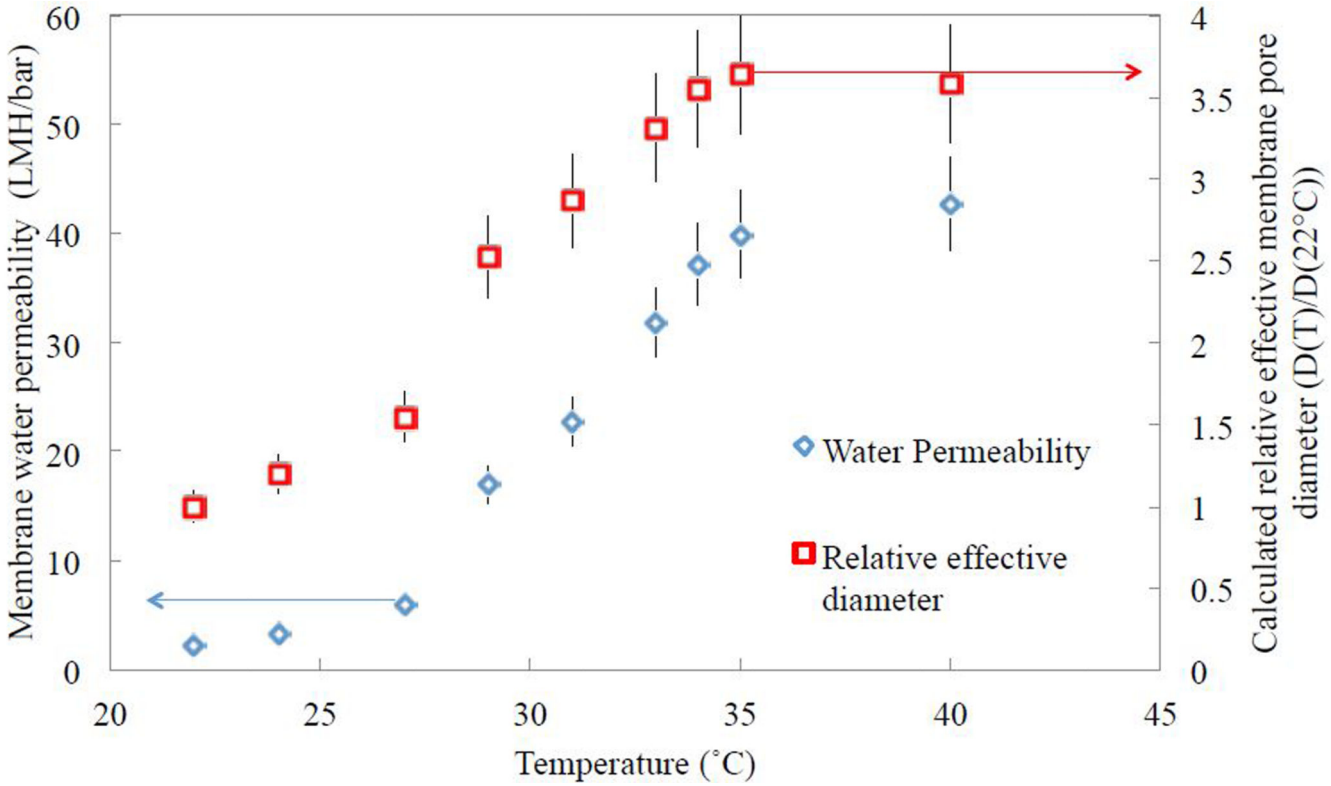

Figure 4:

The effect of temperature on the viscosity-corrected water permeation and effective membrane pore size of a PNIPAm-functionalized PVDF membrane (15 wt% PNIPAm in water, 3 mol% Bisacrylamide crosslinker relative to NIPAm, 2 mol% APS initiator, area of 45 cm^2). As temperature is gradually increased form 22 °C to 41°C at 3.5 bar, a sharp permeance increase (approximately 2-fold) occurs between 28 °C and 34 °, and relative effective membrane pore opening increases over 3-fold for the temperature range.

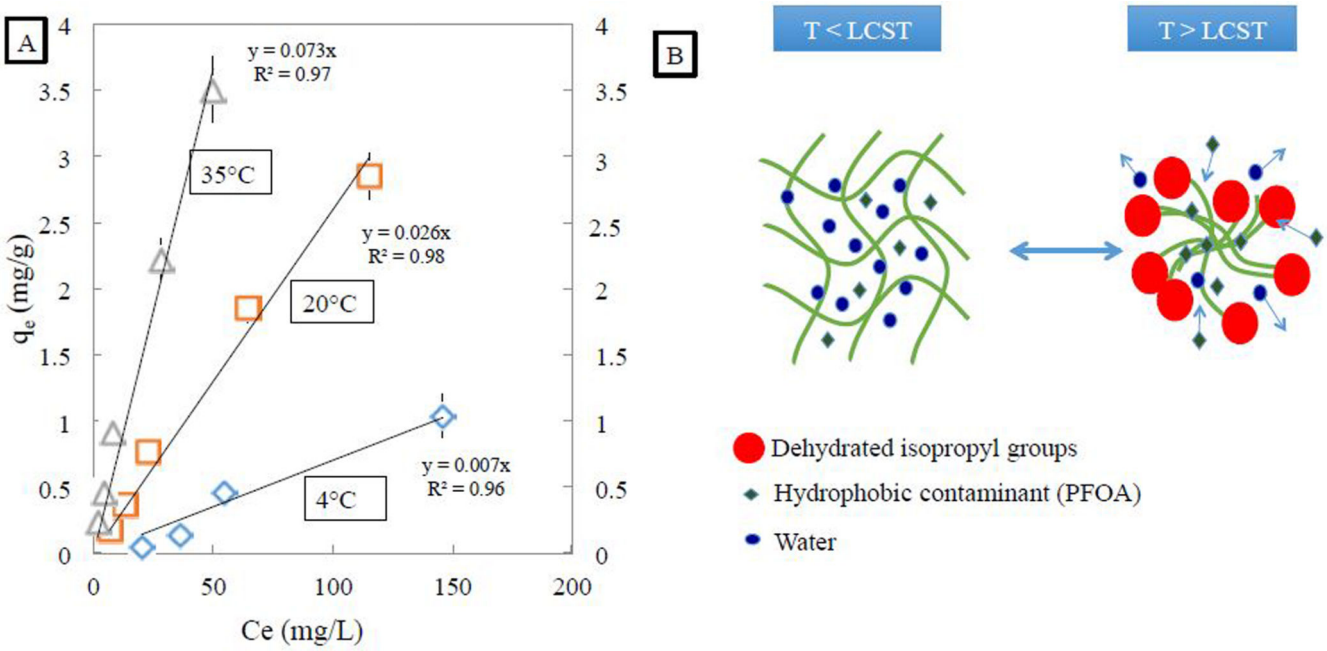

Figure 5:

(A) Adsorption isotherms of PFOA onto PNIPAm hydrogels in water. Initial aqueous PFOA samples had concentrations ranging from 25 mg/L to 250 mg/L, with 0.5g of PNIPAm hydrogels (13 wt% NIPAm, 3 mol% BIS crosslinker, 2 mol% APS) and shaken at 100 rpm until equilibrium. Experimental data is fitted with Freundlich isotherms. (B) Schematic of adsorption of hydrophobic contaminants onto PNIPAm hydrogels in water above PNIPAm's LCST, where PFOA's hydrophobic tail preferentially resides in the dehydrated isopropyl groups of PNIPAm.

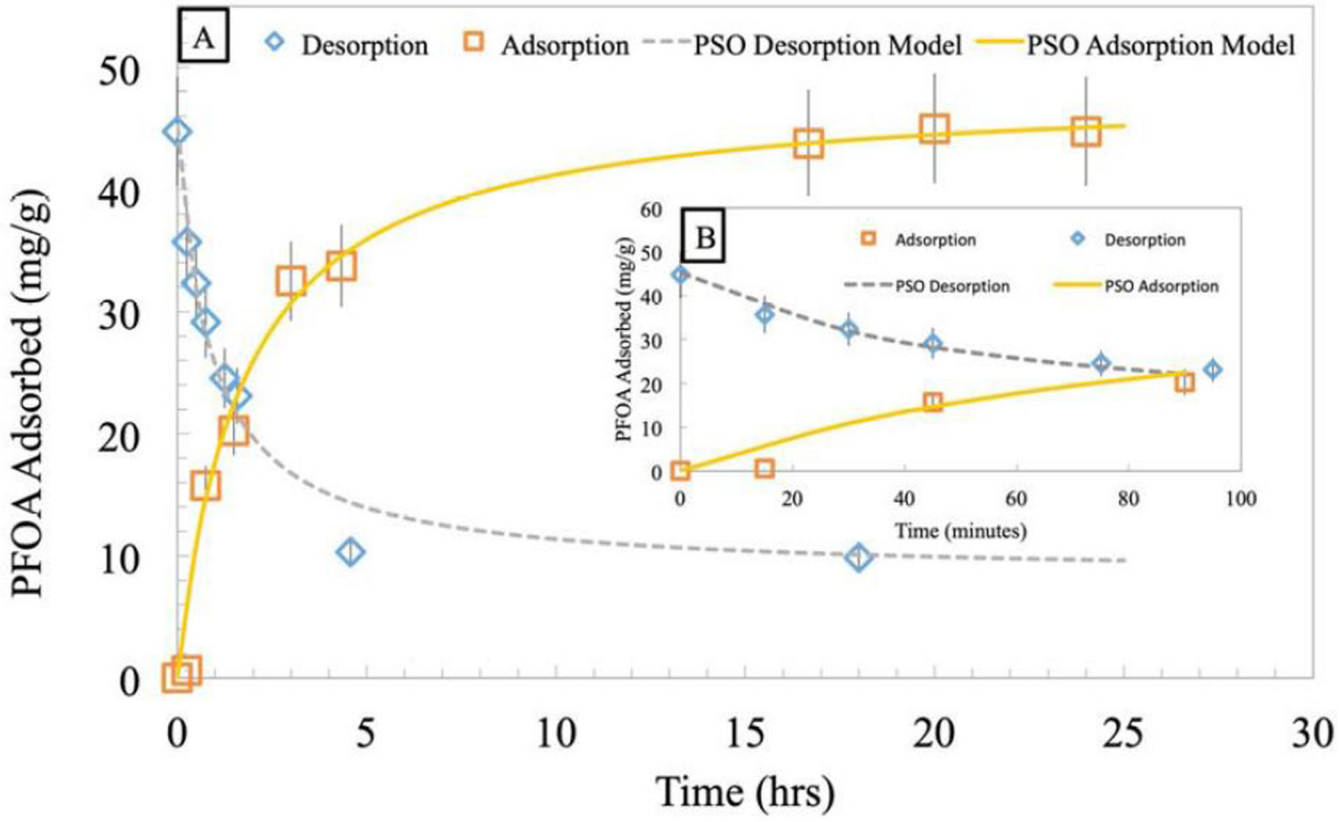

Figure 6:

Adsorption (35 °C) and desorption (20 °C) of PFOA using 2 g of PNIPAm hydrogels (d=1000 nm at 20 °C) in 500 mL of water with initial concentration of 1000 mg/L. PSO model was fit to the experimental data. (A) PFOA adsorption and desorption over one day and (B) Zoomed in PFOA adsorption and desorption for the first 100 minutes.

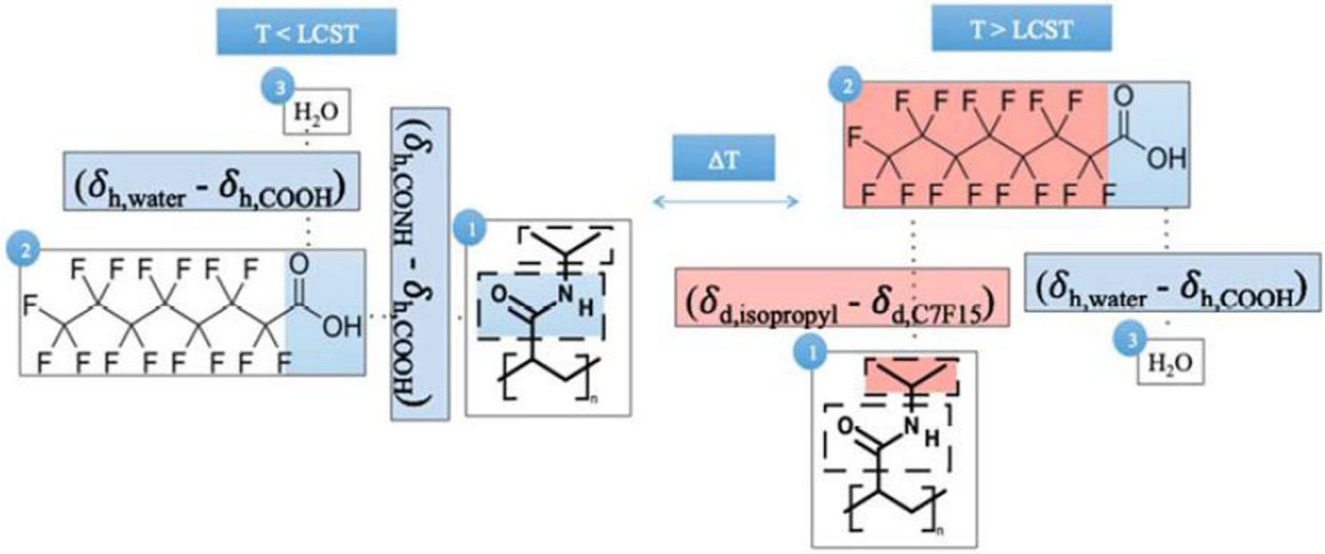

Figure 7:

Schematic depicting interaction of hydrophilic and hydrophobic functional groups for the adsorption and desorption of aqueous PFOA onto PNIPAm, above and below its LCST. The compound labeled 1 refers to PNIPAm, while compounds 2 and 3 refer to PFOA and water respectively. The hydrogen bonding interaction parameters are labeled using δ_h, while the dispersion interaction parameters are labeled using δ_d.

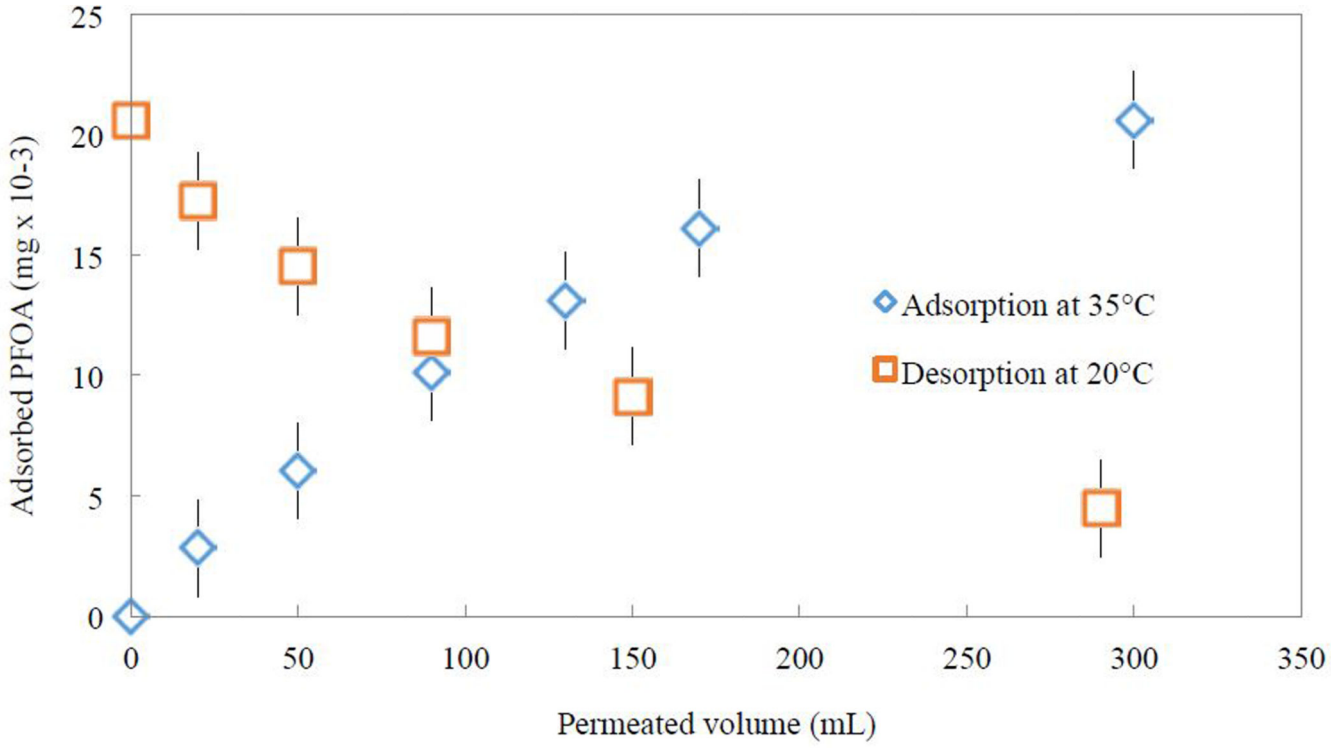

Figure 8:

Adsorption and desorption of PFOA using PNIPAm functionalized PVDF 400 membrane (17% weight gain post polymerization, area of 45 cm^2) by convective flow at constant pressure of 3.5 bar in a dead-end filtration cell. The functionalized membrane adsorbed 20 μg after 300 mL of 0.5 mg/L aqueous PFOA was permeated at 35 °C. 80% of adsorbed PFOA was desorbed after 300 mL of pure DIUF water was permeated.

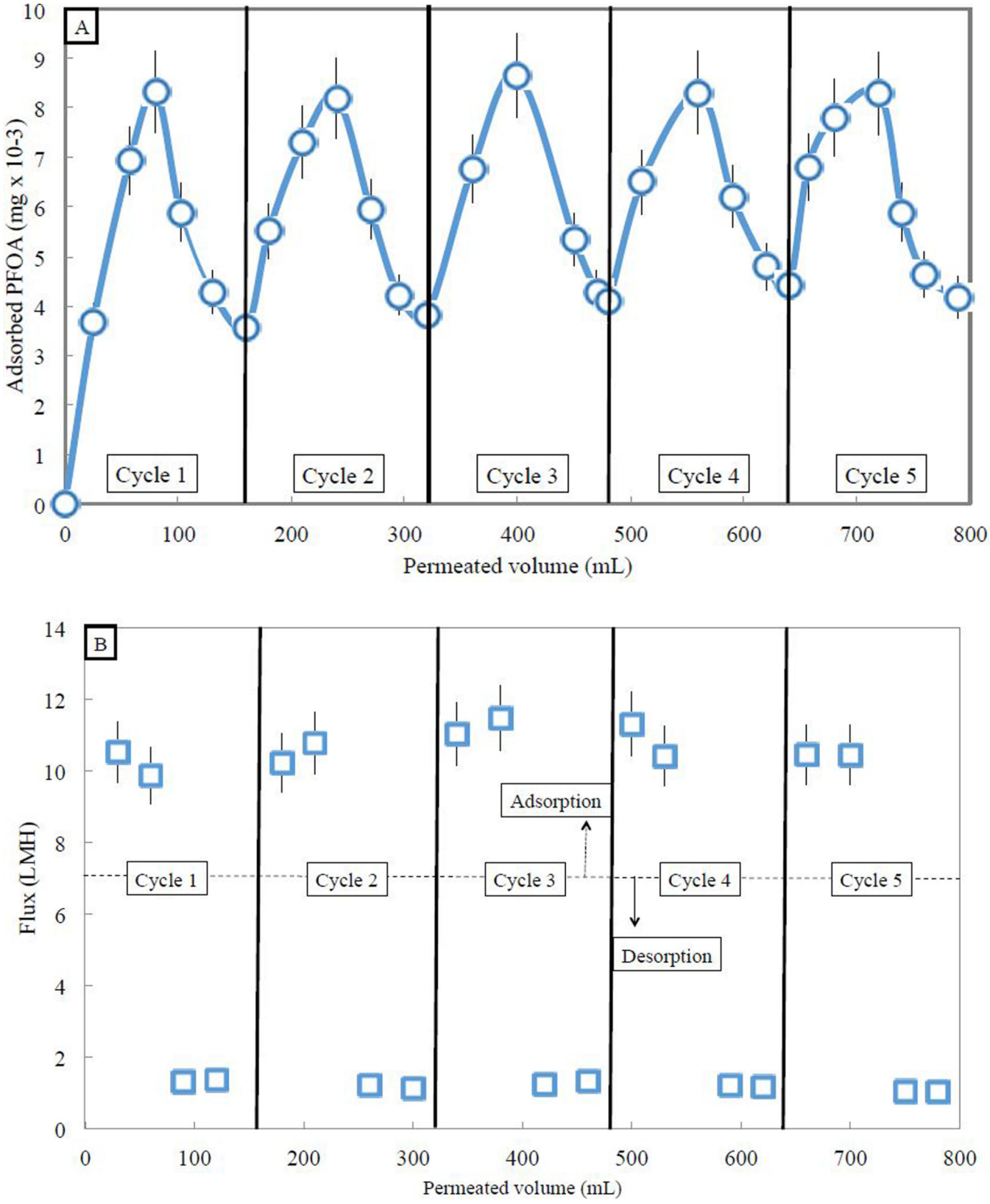

Figure 9:

Adsorption and desorption of PFOA using PNIPAm functionalized PVDF 400 membrane (17% weight gain post polymerization, area of 45 cm^2) by convective flow over five adsorption/desorption cycles of 0.5 mg/L aqueous PFOA solution followed by pure water, at constant pressure of 3.5 bar. (A) Five adsorption/desorption cycles demonstrate consistent temperature swing adsorption. (B) Average flux above LCST is 10.6 LMH, while flux below LCST is 1.2 LMH, and is not affected by the presence of PFOA.

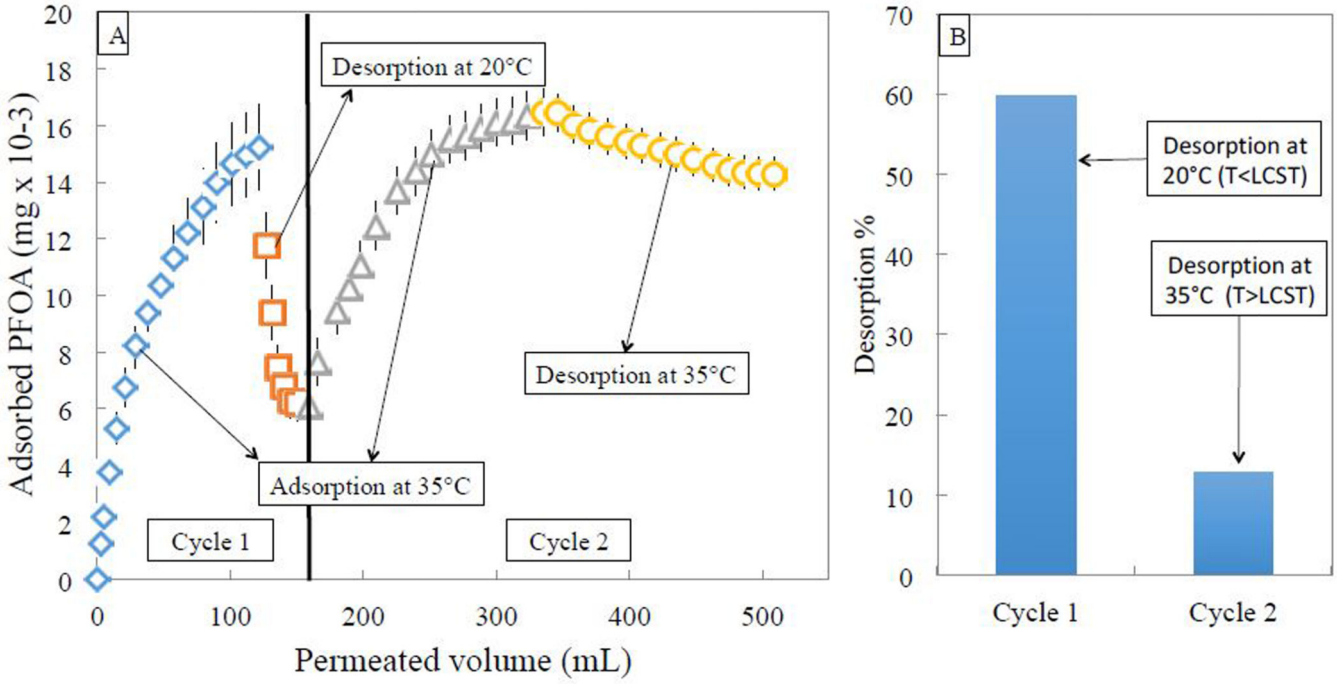

Figure 10:

(A) Two adsorption/desorption cycles of PFOA using PNIPAm functionalized PVDF 700 membrane (15% weight gain post polymerization, area of 45 cm^2) by convective flow at constant pressure of 2.75 bar. Desorption in cycle 1 was conducted at 20 °C compared to 35 °C in cycle 2, both with pure DIUF. (B) Comparison of desorption percentage using pure water at 20°C versus pure water at 35 °C shows much higher desorption using pure water at 20 °C as expected from LCST behavior.

Table 1:

Pseudo-second order adsorption/desorption kinetic rate values derived from experimental data

Temperature	q_e (mg/g)	k_2 (g/mg/h)	ϑ_0 (mg/g/h)	R^2
35 °C	48	0.012	28	0.99
20 °C	11	0.31	41	0.99

Table 2:

EDS elemental ratio analysis of PFOA (A) and of the PNIPAm hydrogel with adsorbed PFOA (B)

(A) PFOA		(B) PNIPAm hydrogel with PFOA	
Element	**At %**	**Element**	**At %**
F	62.0	C	66.4
C	28.8	N	18.7
Na	7.2	O	14.3
O	2.0	F	0.49

Table 3:

Freundlich distribution coefficients of PFOA and PFOS onto PNIPAm hydrogels above and below PNIPAm's LCST

	K_d at 20 °C (L/g)	K_d at 35 °C (L/g)
PFOA	0.026	0.073
PFOS	0.041	0.047